Chapter 1

Robust Adaptive Controls of a Vehicle Seat Suspension System

Do Xuan Phu, Ta Duc Huy and Seung Bok Choi

Additional information is available at the end of the chapter

http://dx.doi.org/10.5772/intechopen.71422

Abstract

This work proposes two novel adaptive fuzzy controllers and applies them to vibration control of a vehicle seat suspension system subjected to severe road profiles. The first adaptive controller is designed by considering prescribed performance of the sliding surface and combined with adaptation laws so that robust stability is guaranteed in the presence of external disturbances. As for the second adaptive controller, both the H-infinity controller and sliding mode controller are combined using inversely fuzzified values of the fuzzy model. In order to evaluate control performances of the proposed two adaptive controllers, a semi-active vehicle suspension system installed with a magneto-rheological (MR) damper is adopted. After determining control gains, two controllers are applied to the system and vibration control performances such as displacement at the driver's position are evaluated and presented in time domain. In this work, to demonstrate the control robustness two severe road profiles of regular bump and random step wave are imposed as external disturbances. It is shown that both adaptive controllers can enhance ride comfort of the driver by reducing the displacement and acceleration at the seat position. This excellent performance is achieved from each benefit of each adaptive controller; accurate tracking performance of the first controller and fast convergence time of the second controller.

Keywords: adaptive fuzzy control, sliding mode control, H-infinity control, prescribed performance of the sliding surface, vibration control, seat suspension system

1. Introduction

Nowadays, modern control-based technical devices such as robotics, assistive machines and home appliances are popularly used to improve the level of human being's life. In these devices,

control algorithm is one of the most important components which brings comfortable requirements to the consumer. The development of control algorithms in recent years is abundantly being undertaken from the aspect of classical control to salient characteristics of intelligent control. The classical control methods are frequently combined with modern control technique to resolve parameter uncertainties and disturbances those are existed in most of control devices. A controller which is formulated using more than two different control schemes is called "a hybrid controller" or "composite controller" [1, 2]. Among many candidates of the hybrid controller, the type of hybrid adaptive controller is the most popular since its structure is relatively simple and its control performance is very robust against the uncertainties or/and external disturbances. A hybrid adaptive control with fuzzy model and wavelet neural networks was presented in [1, 3] in which the sliding mode control was used to connect the parameters of the fuzzy model and the neural networks. This method is the typical model to develop the adaptive control in the last few years. Besides of uncertain nonlinear system, the problem of unknown input nonlinearity such as dead-zone or backlash-like hysteresis was also studied through the hybrid adaptive control [4]. It has been also shown that the neural works can be designed for a good performance of the hybrid adaptive control to deal with the uncertain system [5]. A hybrid adaptive controller possessing the robustness against input and parameter uncertainties was studied using the sliding mode controller associated with the fuzzy model [6, 7]. When a hybrid adaptive controller is formulated, in general the adaptation laws are simultaneously calculated. Furthermore, the back-stepping method was integrated with the fuzzy mode to achieve high performance of the hybrid adaptive controller [8].

As mentioned earlier, both the fuzzy model and the neural networks model are frequently used for the formulation of high performance of a hybrid adaptive controller [9]. Recently, a modified type of the fuzzy model called interval type 2 was combined with the back-stepping method to design of a hybrid adaptive control [10, 11]. It is remarked that the fixed fuzzy model always provides a safe choice in design of a hybrid adaptive control. However, this choice may cause a large error in finding the final values. To resolve this problem, an adaptive interval type 2 fuzzy neural network was developed on the basis of the online technique which can strengthen the flexibility of design parameters against the uncertainties [12]. Besides the above, there are many approaches to formulate new hybrid adaptive controllers such as output feedback control approach to take account for unknown hysteresis [13]. From the aspect of experimental implementation of hybrid adaptive controllers, several dynamic systems featuring magneto-rheological (MR) mount and MR damper are adopted for vibration control [2, 14–18]. Most of hybrid adaptive controllers used in these experimental realizations have been formulated by combining the models of interval type 2 fuzzy and interval type 2 fuzzy neural networks, and the control techniques of H-infinity control and sliding mode control. The advantage of using the interval type 2 fuzzy model is its flexibility in which optimized fuzzy values can be achieved unlike the classical fuzzy rule with the fixed value [19]. In order to improve the fuzzy model, clustering method [20] and data-driven for fuzzy rules [21] were also introduced.

As a subsequent work to develop a new hybrid adaptive controller, in this work two different new hybrid adaptive controllers are developed and their control performances are evaluated by investigation on vibration control of a semi-active seat suspension system installed with MR damper. The first hybrid adaptive controller is designed by combing online interval type 2

fuzzy neural networks model and prescribed performance of the sliding surface associated with adaptation laws to guarantee robust stability (HAC-PP in short). The second hybrid adaptive controller is formulated by combining inversely fuzzified value with H-infinity control to minimize computational cost algorithm (HAC-IFV in short).The stability of both adaptive controllers are rigorously proved based on the Lyapunov stability and appropriate control gains are determined to evaluate vibration control performance. It is shown that both proposed adaptive controllers are very effective and robust for controlling unwanted vibrations or excitations from the road profiles. These are validated by presenting control results showing significant reduction of both the displacement and acceleration at the seat position subjected to external excitations.

2. Formulation of HAC-PP

As mentioned in Introduction, the online interval type 2 fuzzy neural networks (OIT2FNN in short) model is used to formulate two adaptive controllers. The rule base of OIT2FNN can be expressed as follows [22].

$$R_f^j : \text{If } h_1 \text{ is } \mathbf{H}_{f\mathbf{1}}^{\mathbf{j}} \text{ and} \ldots \text{and } h_n \text{ is } \mathbf{H}_{f\mathbf{n}}^{\mathbf{j}} \text{ Then } g \text{ is } a_0^j + \sum_{i=1}^{n} a_i^j h_i \tag{1}$$

where, $\mathbf{H}_{f\mathbf{i}}^{\mathbf{j}}(i = 1, \ldots, n; j = 1, \ldots, m)$ are fuzzy sets, m is the number of rules, and a_i^j are interval sets. The calculation process of OIT2FNN is clearly explained in [22]. The defuzzified output is then determined by

$$g_f = \frac{g_l + g_r}{2} = \frac{\boldsymbol{\theta}_l^T \boldsymbol{\xi}_l^f + \boldsymbol{\theta}_r^T \boldsymbol{\xi}_r^f}{2} \tag{2}$$

In the above, $\boldsymbol{\theta}_l^T = \left[w_1^l \; w_2^l \; w_3^l \ldots w_n^l\right]$ and $\boldsymbol{\theta}_r^T = \left[w_1^r \; w_2^r \; w_3^r \ldots w_n^r\right]$ are the weighting vectors, which symbolize the relation of the rule layer and type-reduction, and the weighted firing strength vectors given by

$$\boldsymbol{\xi}_l^f = \left[\frac{f\_1}{\sum_{i=1}^{n} f\_i} \; \frac{f\_2}{\sum_{i=1}^{n} f\_i} \; \frac{f\_3}{\sum_{i=1}^{n} f\_i} \ldots \frac{f\_n}{\sum_{i=1}^{n} f\_i}\right]^{\mathrm{T}}, \boldsymbol{\xi}_r^f = \left[\frac{\bar{f}_1}{\sum_{i=1}^{n} \bar{f}_i} \; \frac{\bar{f}_2}{\sum_{i=1}^{n} \bar{f}_i} \; \frac{\bar{f}_3}{\sum_{i=1}^{n} \bar{f}_i} \ldots \frac{\bar{f}_n}{\sum_{i=1}^{n} \bar{f}_i}\right]^{T}$$

As a problem formulation, consider a single-input and single-output (SISO) nonlinear system governed by the following equation:

$$\dot{\mathbf{x}} = \mathbf{f}(\mathbf{x}) + \mathbf{g}(\mathbf{x})u(t) + \mathbf{d}(\mathbf{t}) \tag{3}$$

where $\mathbf{f}(\mathbf{x}) \in R^n$ and $\mathbf{g}(\mathbf{x}) \in R^n$ are two unknown non-linear function vectors, $u(t) \in R^1$ is control function, $\mathbf{d}(\mathbf{t}) \in R^n$ is an external disturbance vector, $|\mathbf{d}(\mathbf{t})| \leq \boldsymbol{\delta}\mathbf{d}$ where $\boldsymbol{\delta}\mathbf{d} \in R^n$ is upper bound

of **d**(**t**), $\mathbf{x} = [x_1, x_2, \ldots, x_n] = \left[x_1, \dot{x}_1, \ldots, x_1^{(n-1)}\right]^T \in R^n$ is the state vector of the system. The first sliding surface s_s is defined as follows:

$$s_s = k_1x_1 + k_2x_2 + k_3x_3 + \ldots + k_nx_n = \sum_{i=1}^{n} k_ix_i \tag{4}$$

where, $\mathbf{K} = [k_n, k_{n-11}, k_{n-2}, \ldots, k_1]$ is defined as the coefficients such that all of the roots of the polynomial $\sigma^n + k_{n-1}\sigma^{n-1} + k_{n-2}\sigma^{n-2} + \ldots + k_1$ are in the open left-half complex plane. The sliding surface (4) is rewritten using the state variables as follows:

$$x_n = -k_1x_1 - k_2x_2 - k_3x_3 - \ldots - k_{n-1}x_{n-1} + s_s \tag{5}$$

A new vector $\tilde{\mathbf{x}}$ is defined by $\tilde{\mathbf{x}} = [x_1\ x_2\ x_3 \ldots x_{n-1}]^T$, and thus the system (3) is rewritten as follows:

$$\dot{\tilde{\mathbf{x}}} = \mathbf{S}_1\tilde{\mathbf{x}} + \mathbf{S}_2^T s_s \tag{6}$$

where,

$$\mathbf{S}_1 = \begin{bmatrix} 0 & 1 & 0 & \ldots & 0 \\ 0 & 0 & 1 & \ldots & 0 \\ . & . & . & \ldots & . \\ -k_1 & -k_2 & -k_3 & \ldots & -k_{n-1} \end{bmatrix}, \mathbf{S}_2 = \begin{bmatrix} 0 \\ 0 \\ . \\ 1 \end{bmatrix}$$

The tracking error is defined as $e = x_1 - x_d$ with the desired states of x_d. Then the error performance function is defined as follows [23]:

$$\lambda(t) = (\lambda(0) - \lambda_\infty)e^{-lt} + \lambda_\infty \tag{7}$$

where, $l > 0, 0 < |e(0)| < \lambda(0), \lambda_\infty > 0, \lambda_\infty < \lambda(0)$ then $\lambda_t > 0$ and $\lambda(t)$ tend to λ_∞ exponentially. In order to guarantee fast convergence of tracking error, and obtain a certain convergence accuracy, the tracking error is set as follows:

$$e(t) = \lambda(t)S(\phi) \tag{8}$$

In the above, the prescribed error performance function $S(\phi)$ found as follows:

$$S(\phi) = \frac{e(t)}{\lambda(t)} \tag{9}$$

The function $S(\phi)$ must satisfy the following conditions.

(i) $S(\phi)$ is smooth continuous and monotone increasing function

$$\text{(ii)} -1 < S(\phi) < 1 \tag{10}$$

(iii) $\lim_{\phi \to +\infty} S(\phi) = 1$ and $\lim_{\phi \to -\infty} S(\phi) = -1$

From the above conditions (10), the function $S(\phi)$ can be determined as follows:

$$S(\phi) = \frac{e^{\phi} - e^{-\phi}}{e^{\phi} + e^{-\phi}} \tag{11}$$

Then using Eq. (8), the tracking error is obtained by

$$-\lambda(t) < \lambda(t)S(\phi) < \lambda(t) \Leftrightarrow -\lambda(t) < e(t) < \lambda(t) \tag{12}$$

Hence, the tracking error can be summarized as $\Xi = \{e \in R : |e(t)| < \lambda \ \ \forall t \geq 0$ and $e(t) < \lambda_{\infty}$ for $t \to \infty\}$. On the other hand, the inverse function of (11) is expressed as:

$$\phi = \frac{1}{2}\ln\frac{1+S}{1-S} = \frac{1}{2}\ln\frac{1+(e/\lambda)}{1-(e/\lambda)} = \frac{1}{2}\ln\frac{\lambda+e}{\lambda-e} = \frac{1}{2}[\ln(\lambda+e) - \ln(\lambda-e)] \tag{13}$$

Hence, the derivatives of Eq. (13) are obtained as:

$$\dot{\phi} = \frac{1}{2}\left[\frac{\dot{\lambda}+\dot{e}}{\lambda+e} - \frac{\dot{\lambda}-\dot{e}}{\lambda-e}\right] \tag{14}$$

$$\ddot{\phi} = M_1 + M_2 + M_3\ddot{e} \tag{15}$$

where,

$$M_1 = \frac{\ddot{\lambda}(\lambda+e) - (\dot{\lambda}+\dot{e})^2}{2(\lambda+e)^2}, M_2 = -\frac{\ddot{\lambda}(\lambda-e) - (\dot{\lambda}-\dot{e})^2}{2(\lambda-e)^2}, M_3 = \left(\frac{\lambda+e}{2(\lambda+e)^2} + \frac{\lambda-e}{2(\lambda-e)^2}\right).$$

In order to realize $\phi \to 0$, the second sliding surface is defined as follows:

$$\sigma_s = \dot{\phi} + c_s\phi \tag{16}$$

where $c_s > 0$. The derivative of Eq. (16) is obtained as:

$$\dot{\sigma}_s = \ddot{\phi} + c_s\dot{\phi} = M_1 + M_2 + M_3(f(x) + g(x)u(t) + d(t) - \ddot{x}_d) + c_s\dot{\phi} \tag{17}$$

The lumped uncertainty of system is defined as:

$$w = M_3\tilde{\gamma}_f\xi_f + M_3\tilde{\gamma}_g\xi_g u + M_3 d(t) \tag{18}$$

where $\gamma_f = f(x) - f^*(x)$, $\gamma_g = g(x) - g^*(x)$. Using Eqs. (17) and (18), the derivative Eq. (17) is rewritten as:

$$\dot{\sigma}_s = M_1 + M_2 + M_3 f^*(x) + M_3 g^*(x)u(t) - M_3\ddot{x}_d + c_s\dot{\phi} + w \tag{19}$$

Based on Eq. (2), the relationship between Eq. (19) and OIT2FNN is expressed as follows:

$$\dot{\sigma}_s = M_1 + M_2 + M_3\theta_f{}^*\xi_f + M_3\theta_g{}^*\xi_g u - M_3\ddot{x}_d + c_s\dot{\phi} + w \tag{20}$$

where

$\theta_f^* = \arg\min_{\theta_f \in \Delta\theta_f}\left[\sup_{x\in\Delta x}|f(x) - f^*(x)|\right]$, $\theta_g^* = \arg\min_{\theta_g \in \Delta\theta_g}\left[\sup_{x\in\Delta x}|g(x) - g^*(x)|\right]$, $\Delta\theta_f = \{\theta_f \in R^n, \|\theta_f\| \le \Theta_f\}$, $\Delta\theta_g = \{\theta_g \in R^n, \|\theta_g\| \le \Theta_g\}$, $\Delta x = \{x \in R^n, \|x\| \le \Theta_x\}$

Now, an equivalent control is determined from Eq. (20) based on the assumption $\dot{\sigma}_s \approx 0$:

$$u_1 = \frac{1}{M_3\widehat{\theta}_g\xi_g}\left(-M_1 - M_2 - M_3\widehat{\theta}_f\xi_f + M_3\ddot{x}_d - c_s\dot{\phi}\right) \tag{21}$$

The equivalent control u_1 cannot control the system because it cannot compensate the error from the fuzzy approximation. To guarantee the robustness and stability in control, a robust control part u_2 should be introduced as follows:

$$u_2 = \frac{1}{M_3\widehat{\theta}_g\xi_g}\left(-\sum_{i=1}^{n-1}P_{(n-1)i}x_i - \frac{\sigma_s}{\beta} + \frac{1}{2}M_3\Gamma\xi_z\tilde{\mathbf{x}}\mathbf{P}\mathbf{S}_2\mathbf{S}_2^T\mathbf{P}\tilde{\mathbf{x}}^T\right) \tag{22}$$

Then, the total control u of the system is determined as follows:

$$u = u_1 + u_2 \tag{23}$$

The control u_2 is the combination of two sliding surfaces s_s and σ_s. The value Γ is the adaptive parameter where its boundary is given by $\Delta\Gamma = \{\Gamma \in R, \|\Gamma\| \le \Theta_\Gamma, \sigma_s\Gamma\xi_{fz} \le \rho\}$, and Θ_Γ is constant boundary. The matrix $\mathbf{P} = \mathbf{P}^T \ge 0$ in which its result is a solution of Riccati-like equation given by

$$\mathbf{P}\mathbf{S}_1 + \mathbf{S}_1^{\mathbf{T}}\mathbf{P} + \mathbf{Q} - \sigma_s\Gamma\xi_z\mathbf{P}\mathbf{S}_2\mathbf{S}_2^{\mathbf{T}}\mathbf{P} + \rho\mathbf{P}\mathbf{S}_2\mathbf{S}_2^{\mathbf{T}}\mathbf{P} = 0 \tag{24}$$

where, $\rho \ge \sigma_s\Gamma\xi_z$, ρ is the prescribed attenuation level, $\mathbf{Q} = \mathbf{Q}^{\mathbf{T}} \ge 0$, ξ_z is consequent membership value of the OIT2FNN. When the value $\rho = \sigma_s\Gamma\xi_z$, the Riccati-like equation is rewritten as:

$$\mathbf{P}\mathbf{S}_1 + \mathbf{S}_1^{\mathbf{T}}\mathbf{P} + \mathbf{Q} = 0 \tag{25}$$

Now, Eq. (20) can be analyzed as follows:

$$\dot{\sigma}_s = M_1 + M_2 + M_3\tilde{\gamma}_f\xi_f + M_3\tilde{\gamma}_g\xi_g u - M_3\ddot{x}_d + c_s\dot{\phi} + w + \left[M_3\widehat{\theta}_f\xi_f + M_3\widehat{\theta}_g\xi_g u\right] \tag{26}$$

where $\tilde{\gamma}_f = \theta_f{}^* - \widehat{\theta}_f$, $\tilde{\gamma}_g = \theta_g{}^* - \widehat{\theta}_g$. Using Eqs. (23) and (26), Eq. (26) is rewritten by

$$\dot{\sigma}_s = \left[-\sum_{i=1}^{n-1}P_{(n-1)i}x_i - \frac{\sigma_s}{\beta} + \frac{1}{2}M_3\Gamma\xi_z\tilde{\mathbf{x}}\mathbf{P}\mathbf{S}_2\mathbf{S}_2^T\mathbf{P}\tilde{\mathbf{x}}^T\right] + \left[M_3\tilde{\gamma}_f\xi_f + M_3\tilde{\gamma}_g\xi_g u + w\right] \tag{27}$$

Now, the stability of the proposed adaptive control system can be solidly proved with Eqs. (21)–(23) and adaptation laws as follows:

$$\dot{\tilde{\gamma}}_f = -\mu_1 M_3 \sigma_s \xi_f; \;\; \dot{\tilde{\gamma}}_g = -\mu_2 M_3 \sigma_s \xi_g u; \;\; \dot{\Gamma} = -\mu_3 M_3 \sigma_s \xi_z \tilde{\mathbf{x}} \mathbf{P} \mathbf{S}_2 \mathbf{S}_2^T \mathbf{P} \tilde{\mathbf{x}}^T \tag{28}$$

In order to make a proof, in this work the following Lyapunov function candidate is proposed.

$$L_v = \frac{1}{2}\sigma^2{}_s + \frac{1}{2}\tilde{\mathbf{x}}\mathbf{P}\tilde{\mathbf{x}}^T + \frac{1}{2\mu_1}\tilde{\gamma}^2{}_f + \frac{1}{2\mu_2}\tilde{\gamma}^2{}_g + \frac{1}{2\mu_3}\Gamma^2 \tag{29}$$

The derivative of Eq. (29) is then obtained by

$$\dot{L}_v = \sigma_s \dot{\sigma}_s + \frac{1}{2}\tilde{\mathbf{x}}\mathbf{P}\dot{\tilde{\mathbf{x}}}^T + \frac{1}{2}\tilde{\mathbf{x}}\mathbf{P}\dot{\tilde{\mathbf{x}}}^T + \frac{1}{\mu_1}\tilde{\gamma}_f\dot{\tilde{\gamma}}_f + \frac{1}{\mu_2}\tilde{\gamma}_g\dot{\tilde{\gamma}}_g + \frac{1}{\mu_3}\Gamma\dot{\Gamma} \tag{30}$$

Substituting Eq. (27) into Eq. (30), Eq. (30) is rewritten as follows:

$$\begin{aligned}\dot{L}_v = &\left[M_3\sigma_s\tilde{\gamma}_f\xi_f + \frac{1}{\mu_1}\tilde{\gamma}_f\dot{\tilde{\gamma}}\right] + \left[M_3\sigma_s\tilde{\gamma}_g\xi_g u + \frac{1}{\mu_2}\tilde{\gamma}_g\dot{\tilde{\gamma}}_g\right] \\ &+ \left[M_3\Gamma\xi_z\sigma_s\tilde{\mathbf{x}}\mathbf{P}\mathbf{S}_2\mathbf{S}_2^T\mathbf{P}\tilde{\mathbf{x}}^T + \frac{1}{\mu_3}\Gamma\dot{\Gamma}\right] + \left[\sigma_s w - \frac{\sigma^2{}_s}{\beta} - \frac{1}{2}\rho\mathbf{P}\mathbf{S}_2\mathbf{S}_2^T\mathbf{P} - \frac{1}{2}\tilde{\mathbf{x}}^T\mathbf{Q}\tilde{\mathbf{x}}^T\right]\end{aligned} \tag{31}$$

It is noted that Eq. (24) is used in finding Eq. (31). Substituting Eq. (28) into Eq. (31), the following is achieved.

$$\dot{L}_v = \left[-\frac{1}{2}\tilde{\mathbf{x}}^T\mathbf{Q}\tilde{\mathbf{x}}^T - \frac{1}{2}\left(\frac{\sigma_s}{\sqrt{\beta}} - \sqrt{\beta}w\right)^2 + \beta w^2\right] - \frac{1}{2}\rho\mathbf{P}\mathbf{S}_2\mathbf{S}_2^T\mathbf{P} \leq -\frac{1}{2}\tilde{\mathbf{x}}^T\mathbf{Q}\tilde{\mathbf{x}}^T + \beta w^2 \tag{32}$$

Eq. (32) cannot use for conclusion of stability. Hence, it will be integrated from $t=0$ to $t=T$, we have:

$$L_v(0) - L_v(T) + \beta\int_0^T w^2 dt \geq \frac{1}{2}\int_0^T \tilde{\mathbf{x}}\mathbf{Q}\tilde{\mathbf{x}}^T dt \tag{33}$$

where, $L_v(0) = \frac{1}{2}\sigma^2{}_s(0) + \frac{1}{2}\tilde{\mathbf{x}}(0)\mathbf{P}\tilde{\mathbf{x}}^T(0) + \frac{1}{2\mu_1}\tilde{\gamma}^2{}_f(0) + \frac{1}{2\mu_2}\tilde{\gamma}^2{}_g(0) + \frac{1}{2\mu_3}\Gamma^2(0)$. The value $L_v(T)$ is always positive, so Eq. (33) is determined as:

$$L_v(0) + \beta\int_0^T w^2 dt \geq \frac{1}{2}\int_0^T \tilde{\mathbf{x}}\mathbf{Q}\tilde{\mathbf{x}}^T dt \geq 0 \tag{34}$$

From Eqs. (32) and (34), the stability is guaranteed.

From the boundedness of the parameters $\tilde{\gamma}_f$ and $\tilde{\gamma}_g$, the closed sets are defined as $\Xi_1 = \left\{\tilde{\gamma}_f \middle| \left\|\tilde{\gamma}_f\right\| \leq \aleph_f\right\}$, $\Xi_2 = \left\{\tilde{\gamma}_g \middle| \left\|\tilde{\gamma}_g\right\| \leq \aleph_g\right\}$, $\Xi_{\delta 1} = \left\{\tilde{\gamma}_f \middle| \left\|\tilde{\gamma}_f\right\| \leq \aleph_f + \delta_1\right\}$, $\Xi_{\delta 2} = \left\{\tilde{\gamma}_g \middle| \left\|\tilde{\gamma}_g\right\| \leq \aleph_g + \delta_2\right\}$.

In here, $\aleph_f$, $\aleph_g$, δ_1, δ_2 are the choosing parameters. Hence, the adjusted adaptation laws are redefined as follows:

$$\dot{\tilde{\gamma}}_f = \begin{cases} -\mu_1 M_3 \sigma_s \xi_f & \text{if } \left\|\tilde{\gamma}_{\mathrm{f}}\right\| < \aleph_f \text{ or } \left(\left\|\tilde{\gamma}_{\mathrm{f}}\right\| = \aleph_f \text{ and } M_3 \sigma_s \xi_f \tilde{\gamma}_{\mathrm{f}} \geq 0\right) \\ -\mu_1 M_3 \sigma_s \xi_f + \mu_1 \dfrac{\left(\left\|\tilde{\gamma}_f\right\|^2 - \aleph_f\right) M_3 \sigma_s \xi_f \tilde{\gamma}_f}{\delta_1 \left\|\tilde{\gamma}_f\right\|^2} & \text{if } \left\|\tilde{\gamma}_{\mathrm{f}}\right\| = \aleph_f \text{ and } M_3 \sigma_s \xi_f \tilde{\gamma}_{\mathrm{f}} < 0 \end{cases} \tag{35}$$

$$\dot{\tilde{\gamma}}_g = \begin{cases} -\mu_2 M_3 \sigma_s \xi_g u & \text{if } \left\|\tilde{\gamma}_{\mathrm{g}}\right\| < \aleph_g \text{ or } \left(\left\|\tilde{\gamma}_{\mathrm{g}}\right\| = \aleph_g \text{ and } M_3 \sigma_s \xi_g u \tilde{\gamma}_{\mathrm{g}} \geq 0\right) \\ -\mu_2 M_3 \sigma_s \xi_g u + \mu_2 \dfrac{\left(\left\|\tilde{\gamma}_g\right\|^2 - \aleph_g\right) M_3 \sigma_s \xi_g u \tilde{\gamma}_g}{\delta_2 \left\|\tilde{\gamma}_g\right\|^2} & \text{if } \left\|\tilde{\gamma}_{\mathrm{g}}\right\| = \aleph_g \text{ and } M_3 \sigma_s \xi_g u \tilde{\gamma}_{\mathrm{g}} < 0 \end{cases} \tag{36}$$

$$\dot{\Gamma} = \begin{cases} -\mu_3 M_3 \sigma_s \xi_z \tilde{\mathbf{x}} \mathbf{P} \mathbf{S}_2 \mathbf{S}_2^T \mathbf{P} \tilde{\mathbf{x}}^T \text{if } \|\Gamma\| < \Theta_\Gamma \text{ or } \left(\|\Gamma\| = \Theta_\Gamma + \delta_3 \text{ and } M_3 \sigma_s \xi_z \tilde{\mathbf{x}} \mathbf{P} \mathbf{S}_2 \mathbf{S}_2^T \mathbf{P} \tilde{\mathbf{x}}^T \Gamma \geq 0\right) \\ -\mu_3 M_3 \sigma_s \xi_z \tilde{\mathbf{x}} \mathbf{P} \mathbf{S}_2 \mathbf{S}_2^T \mathbf{P} \tilde{\mathbf{x}}^T + \mu_3 \dfrac{\left(\|\Gamma\|^2 - \Theta_\Gamma\right) M_3 \sigma_s \xi_z \tilde{\mathbf{x}} \mathbf{P} \mathbf{S}_2 \mathbf{S}_2^T \mathbf{P} \tilde{\mathbf{x}}^T \Gamma}{\delta_3 \|\Gamma\|^2} \\ \text{if } \|\Gamma\| = \Theta_\Gamma \text{ and } M_3 \sigma_s \xi_z \tilde{\mathbf{x}} \mathbf{P} \mathbf{S}_2 \mathbf{S}_2^T \mathbf{P} \tilde{\mathbf{x}}^T \Gamma < 0 \end{cases} \tag{37}$$

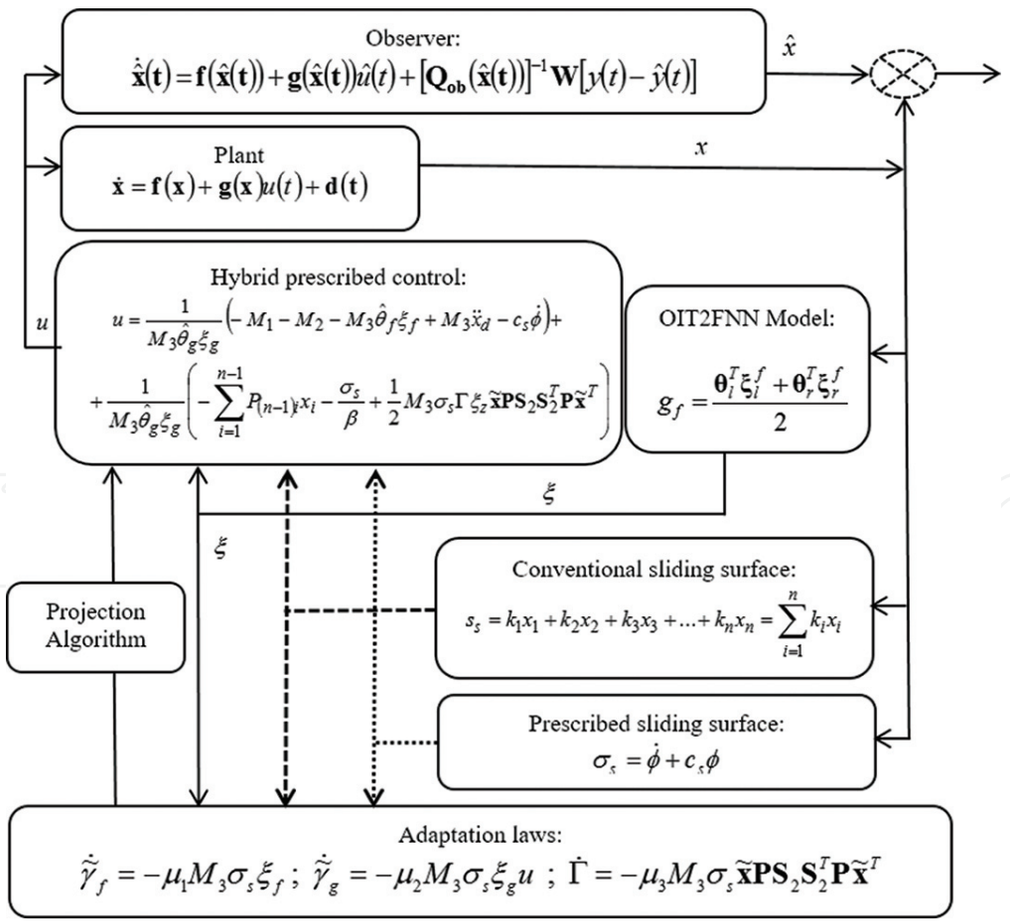

Figure 1. Control flow chart of the HAC-PP.

In the above, δ_1, δ_2 and δ_3 are choosing parameters related boundaries of $f(x)$, $g(x)$ and Γ. It is noted here that in order to utilize the states of the system, the Luenberger observer [24] has been used in this work. **Figure 1** presents a flow chart of the HAC-PP showing the combination of each controller and the prescribed performance.

3. Formulation of HAC-IFV

As a first step to design the controller, consider the system (3) rewritten by

$$\dot{\mathbf{x}} = \mathbf{f_0}(\mathbf{x}) + \mathbf{g_0}(\mathbf{x})u(t) + \mathbf{D} \tag{38}$$

where, the function $\mathbf{f}_0(\mathbf{x})$ and $\mathbf{g}_0(\mathbf{x})$ are the functions of $\mathbf{f}(\mathbf{x})$ and $\mathbf{g}(\mathbf{x})$ which are determined as:

$$\mathbf{f}(\mathbf{x}) = \mathbf{f_0}(\mathbf{x}) + \boldsymbol{\delta}\mathbf{f}(\mathbf{x}); 0 < |\boldsymbol{\delta}\mathbf{f}(\mathbf{x})| < \|\boldsymbol{\delta}\mathbf{f}\|_\infty, \mathbf{g}(\mathbf{x}) = \mathbf{g_0}(\mathbf{x}) + \boldsymbol{\delta}\mathbf{g}(\mathbf{x}); 0 < |\boldsymbol{\delta}\mathbf{g}(\mathbf{x})| < \|\boldsymbol{\delta}\mathbf{g}\|_\infty.$$

$$\mathbf{f_0}(\mathbf{x}) = \left[x_2, \ldots, x_n, f_0\right]^T, \mathbf{g_0}(\mathbf{x}) = \left[0, \ldots, 0, g_0\right]^T, \boldsymbol{\delta}\mathbf{f} = \left[0, 0, \ldots, \delta f_0\right]^T, \boldsymbol{\delta}\mathbf{g} = \left[0, 0, \ldots, \delta g_0\right]^T.$$

In the above, $\boldsymbol{\delta}\mathbf{f}$ and $\boldsymbol{\delta}\mathbf{g}$ are two positive vectors. It is noted that $\mathbf{D} = \boldsymbol{\delta}\mathbf{f} + \boldsymbol{\delta}\mathbf{g}u(t) + \mathbf{d}(\mathbf{t})$ denotes the uncertain disturbance and $\mathbf{D} = [0, 0, \ldots, D_0]^T$. In order to formulate the controller, the following assumption is made: There exists a constant $g_m \in \mathfrak{R}^+$ to satisfy $|g(x)| > g_m$. Without loss of generality, it is assumed that the equation $g(x) > g_m$. The error between a desired output x_d and the measured output x is $e = x_d - x$. Hence, the error vector is defined by $\mathbf{E} = [e_0, e_1, e_2, \ldots, e_n] = \left[e, \dot{e}, \ddot{e}, \ldots, e^{(n-1)}\right]$. The sliding surface s_s can be written as $s(x,t) = \mathbf{K}^T\mathbf{E}$, and its derivative is found as $\dot{s}(x,t) = \mathbf{K}^T\dot{\mathbf{E}} = \mathbf{K}^T\dot{\mathbf{x}}_d - \mathbf{K}^T\dot{\mathbf{x}}$. Using this derivative function of the sliding surface and Eq. (38), the initial control law u is determined by:

$$u = \frac{1}{g_0(x)}\left(-f_0(x) + \dot{x}_d + \mathbf{K^T E} + D_0\right) \tag{39}$$

Assuming the disturbance of $\mathbf{D} \approx 0$, then Eq. (39) can be rewritten as:

$$u = \frac{1}{g_0(x)}\left(-f_0(x) + \dot{x}_d + \mathbf{K^T E}\right) \tag{40}$$

The relationship of Eq. (40) and OIT2FNN is expressed by

$$u = \frac{1}{g_{00}(x)}\left(-f_{00}(x) + \dot{x}_d + \mathbf{K^T E}\right) \tag{41}$$

where, $f_{00}(x)$ and $g_{00}(x)$ are the fuzzified functions of $f(x)$ and $g(x)$, respectively. The derivative of $\mathbf{E}$ is expressed through Eqs. (40) and (41) as follows:

$$\begin{aligned}\dot{\mathbf{E}} &= \dot{\mathbf{x}}_\mathbf{d} - \dot{\mathbf{x}} = \big(g_{00}(x) - g_0(x)\big)u + \big(f_{00}(x) - f_0(x)\big) - \mathbf{K}^\mathbf{T}\mathbf{E} \\ &= \mathbf{S_1}\mathbf{E} + \mathbf{S_2}\big[\big(g_{00}(x) - g(x)\big)u + \big(f_{00}(x) - f(x)\big)\big]\end{aligned} \tag{42}$$

Define the minimum approximation error due to fuzzy approximation as follows.

$$w = \big(f^*{}_{00}(x) - f(x)\big) + \big(g^*{}_{00}(x) - g(x)\big)u \tag{43}$$

Substituting functions of $f_{00}(x)$, $g_{00}(x)$ and (43) into Eq. (42) yields the following equation.

$$\dot{\mathbf{E}} = \mathbf{S_1}\mathbf{E} + \mathbf{S_2}\Big[\Big(\theta_f^* - \theta_f\Big)\xi_f + \Big(\theta_g^* - \theta_g\Big)\xi_g u + w\Big] \tag{44}$$

Let $\gamma_f = \Big(\theta_f^* - \theta_f\Big)$, $\gamma_g = \Big(\theta_g^* - \theta_g\Big)$. From Eq. (44), the equivalence control u_1 established without the minimum approximation error w is defined as follows:

$$u_1 = \frac{1}{\widehat{\gamma}_g \xi_g}\Big(-\widehat{\gamma}_f \xi_f\Big) \tag{45}$$

where, $\widehat{\gamma}_f$ and $\widehat{\gamma}_g$ are the estimates of γ_f and γ_g, respectively. The control u_1 cannot use for control the system because of the error from the fuzzy approximation. To deal with this problem, a new robust compensator based on the inversely fuzzified value is suggested as follows:

$$u_2 = -\frac{1}{\Gamma \xi_z}\mathbf{E}^\mathbf{T}\mathbf{P}\mathbf{S}_2 \tag{46}$$

where, Γ is a constant, and $\mathbf{P} = \mathbf{P}^\mathbf{T} \geq 0$ is the solution of the following Riccati-like equation.

$$\mathbf{P}\mathbf{S_1} + \mathbf{S_1^T}\mathbf{P} + \mathbf{Q} - \frac{1}{\Gamma \xi_z}\mathbf{P}\mathbf{S}_2\mathbf{S}_\mathbf{2}^\mathbf{T}\mathbf{P} + \rho \mathbf{P}\mathbf{S}_2\mathbf{S}_\mathbf{2}^\mathbf{T}\mathbf{P} = 0 \tag{47}$$

where, $\rho \geq \frac{1}{\Gamma \xi_z}$, ρ is the prescribed attenuation level, $\mathbf{Q} = \mathbf{Q}^\mathbf{T} \geq 0$, ξ_z is consequent membership value of the OIT2FNN. When the value $\rho = \frac{1}{\Gamma \xi_z}$, the Riccati-like equation is obtain as given in Eq. (25). It is noteworthy that Eq. (25) is objective to guarantee the stability of the system. If this condition is obtained, the fuzzy approximation error is removed, and then the control u_1 is the main controller to retain the stability of the system. From Eqs. (45) and (46), the final fuzzy control of the system is determined as follows:

$$u = u_1 + u_2 = \frac{1}{\widehat{\gamma}_g \xi_g}\Big(-\widehat{\gamma}_f \xi_f\Big) - \frac{1}{\Gamma \xi_z}\mathbf{E}^\mathbf{T}\mathbf{P}\mathbf{S_2} \tag{48}$$

Now, substituting Eq. (48) into (44) yields he following.

$$\dot{\mathbf{E}} = \mathbf{S_1}\mathbf{E} + \mathbf{S_2}\left[\tilde{\gamma}_f \xi_f + \tilde{\gamma}_g \xi_g u_1 + g_o u_2 + w\right] \tag{49}$$

where, $\tilde{\gamma}_f = \gamma_f - \hat{\gamma}_f$, $\tilde{\gamma}_g = \gamma_g - \hat{\gamma}_g$. Consider the Lyapunov function candidate of the system as follows:

$$V = \frac{1}{2}\mathbf{E}^{\mathbf{T}}\mathbf{P}\mathbf{E} + \frac{1}{2\alpha_1}\tilde{\gamma}_f^2 + \frac{1}{2\alpha_2}\tilde{\gamma}_g^2 \tag{50}$$

The derivative of Eq. (50), and then substituting Eq. (25) into the derivative, the result is obtained as follows:

$$\begin{aligned}\dot{V} = &-\frac{1}{2}\mathbf{E}^{\mathbf{T}}\mathbf{Q}\mathbf{E} - \frac{g_m}{\Gamma\xi_z}\left(\mathbf{E}^{\mathbf{T}}\mathbf{P}\mathbf{S_2}\right)^2 + \mathbf{E}^{\mathbf{T}}\mathbf{P}\mathbf{S_2}w + \frac{1}{\alpha_1}\left(\alpha_1\mathbf{E}^{\mathbf{T}}\mathbf{P}\mathbf{S_2}\xi_f - \dot{\hat{\gamma}}_f\right)\tilde{\gamma}_f \\ &+ \frac{1}{\alpha_2}\left(\alpha_2\mathbf{E}^{\mathbf{T}}\mathbf{P}\mathbf{S_2}\xi_g u_1 - \dot{\hat{\gamma}}_g\right)\tilde{\gamma}_g\end{aligned} \tag{51}$$

From Eq. (51), adaptation laws are established as follows:

$$\dot{\hat{\gamma}}_f = -\alpha_1\mathbf{E}^{\mathbf{T}}\mathbf{P}\mathbf{S_2}\xi_f \tag{52}$$

$$\dot{\hat{\gamma}}_g = -\alpha_2\mathbf{E}^{\mathbf{T}}\mathbf{P}\mathbf{S_2}\xi_g u_1 \tag{53}$$

Applying Eqs. (52) and (53), Eq. (51) can be written as follows:

$$\begin{aligned}\dot{V} &\le -\frac{1}{2}\mathbf{E}^{\mathbf{T}}\mathbf{Q}\mathbf{E} - \frac{g_m}{\Gamma\xi_z}\left(\mathbf{E}^{\mathbf{T}}\mathbf{P}\mathbf{S_2}\right)^2 + \mathbf{E}^{\mathbf{T}}\mathbf{P}\mathbf{S_2}w \\ &= -\frac{1}{2}\mathbf{E}^{\mathbf{T}}\mathbf{Q}\mathbf{E} - \left(\sqrt{\frac{g_m}{\Gamma\xi_z}}\mathbf{E}^{\mathbf{T}}\mathbf{P}\mathbf{S_2} - \frac{w_m}{2\rho}\right)^2 + \frac{1}{4\rho}{w_m}^2 \le -\frac{1}{2}\mathbf{E}^{\mathbf{T}}\mathbf{Q}\mathbf{E} + \frac{1}{4\rho}{w_m}^2\end{aligned} \tag{54}$$

where, $w_m = \frac{w}{\sqrt{g_m}}$.

Now, the integration of (54) from $t=0$ to $t=T$ yields the following equation.

$$V(0) - V(T) + \frac{1}{4\rho}\int_0^T {w_m}^2 dt \ge \frac{1}{2}\int_0^T \mathbf{E}^{\mathbf{T}}\mathbf{Q}\mathbf{E}dt \tag{55}$$

The value of $V(T) \ge 0$, and thus Eq. (55) is rewritten as follows:

$$V(0) + \frac{1}{4\rho}\int_0^T {w_m}^2 dt \ge \frac{1}{2}\int_0^T \mathbf{E}^{\mathbf{T}}\mathbf{Q}\mathbf{E}dt \tag{56}$$

where, $V(0) = \frac{1}{2}\mathbf{E}^{\mathbf{T}}(0)\mathbf{P}\mathbf{E}(0) + \frac{1}{2\alpha_1}\tilde{\gamma}_f^2(0) + \frac{1}{2\alpha_2}\tilde{\gamma}_g^2(0)$. Hence the H-infinity tracking performance is achieved. From the boundedness of the parameters, $\tilde{\gamma}_f$ and $\tilde{\gamma}_g$ are guaranteed by closed sets

defined as $\Omega_1 = \left\{\tilde{\gamma}_f \middle| \left\|\tilde{\gamma}_f\right\| \le \mathfrak{I}_f\right\}$, $\Omega_2 = \left\{\tilde{\gamma}_g \middle| \left\|\tilde{\gamma}_g\right\| \le \mathfrak{I}_g\right\}$, $\Omega_{\delta 1} = \left\{\tilde{\gamma}_f \middle| \left\|\tilde{\gamma}_f\right\| \le \mathfrak{I}_f + \delta_1\right\}$, $\Omega_{\delta 2} = \left\{\tilde{\gamma}_g \middle| \left\|\tilde{\gamma}_g\right\| \le \mathfrak{I}_g + \delta_2\right\}$ where $\mathfrak{I}_f, \mathfrak{I}_g$, δ_1, δ_2 are the choosing parameters. Hence, the adjusted adaptation laws are redefined as follows:

$$\dot{\tilde{\gamma}}_f = \begin{cases} -\alpha_1 \mathbf{E}^{\mathbf{T}} \mathbf{P} \mathbf{S}_2 \xi_f & \text{if } \|\tilde{\gamma}_f\| < \mathfrak{I}_f \text{ or } \left(\|\tilde{\gamma}_f\| = \mathfrak{I}_f \text{ and } \mathbf{E}^{\mathbf{T}} \mathbf{P} \mathbf{S}_2 \xi_f \tilde{\gamma}_f \ge 0\right) \\ -\alpha_1 \mathbf{E}^{\mathbf{T}} \mathbf{P} \mathbf{S}_2 \xi_f + \alpha_1 \dfrac{\left(\left\|\tilde{\gamma}_f\right\|^2 - \mathfrak{I}_f\right) \mathbf{E}^{\mathbf{T}} \mathbf{P} \mathbf{S}_2 \xi_f \tilde{\gamma}_f}{\delta_1 \left\|\tilde{\gamma}_f\right\|^2} & \text{if } \|\tilde{\gamma}_f\| = \mathfrak{I}_f \text{ and } \mathbf{E}^{\mathbf{T}} \mathbf{P} \mathbf{S}_2 \xi_f \tilde{\gamma}_f < 0 \end{cases} \tag{57}$$

$$\dot{\tilde{\gamma}}_g = \begin{cases} -\alpha_2 \mathbf{E}^{\mathbf{T}} \mathbf{P} \mathbf{S}_2 \xi_g u_1 & \text{if } \left\|\tilde{\gamma}_g\right\| < \mathfrak{I}_g \text{ or } \left(\left\|\tilde{\gamma}_g\right\| = \mathfrak{I}_g \text{ and } \mathbf{E}^{\mathbf{T}} \mathbf{P} \mathbf{S}_2 \xi_f u_1 \tilde{\gamma}_g \ge 0\right) \\ -\alpha_2 \mathbf{E}^{\mathbf{T}} \mathbf{P} \mathbf{S}_2 \xi_g u_1 + \alpha_2 \dfrac{\left(\left\|\tilde{\gamma}_g\right\|^2 - \mathfrak{I}_g\right) \mathbf{E}^{\mathbf{T}} \mathbf{P} \mathbf{S}_2 \xi_g u_1 \tilde{\gamma}_g}{\delta_2 \left\|\tilde{\gamma}_g\right\|^2} & \text{if } \left\|\tilde{\gamma}_g\right\| = \mathfrak{I}_g \text{ and } \mathbf{E}^{\mathbf{T}} \mathbf{P} \mathbf{S}_2 \xi_g u_1 \tilde{\gamma}_g < 0 \end{cases} \tag{58}$$

Figure 2 presents a flow chart of the HAC-IFV showing the combination process of each controller with the adaptation laws.

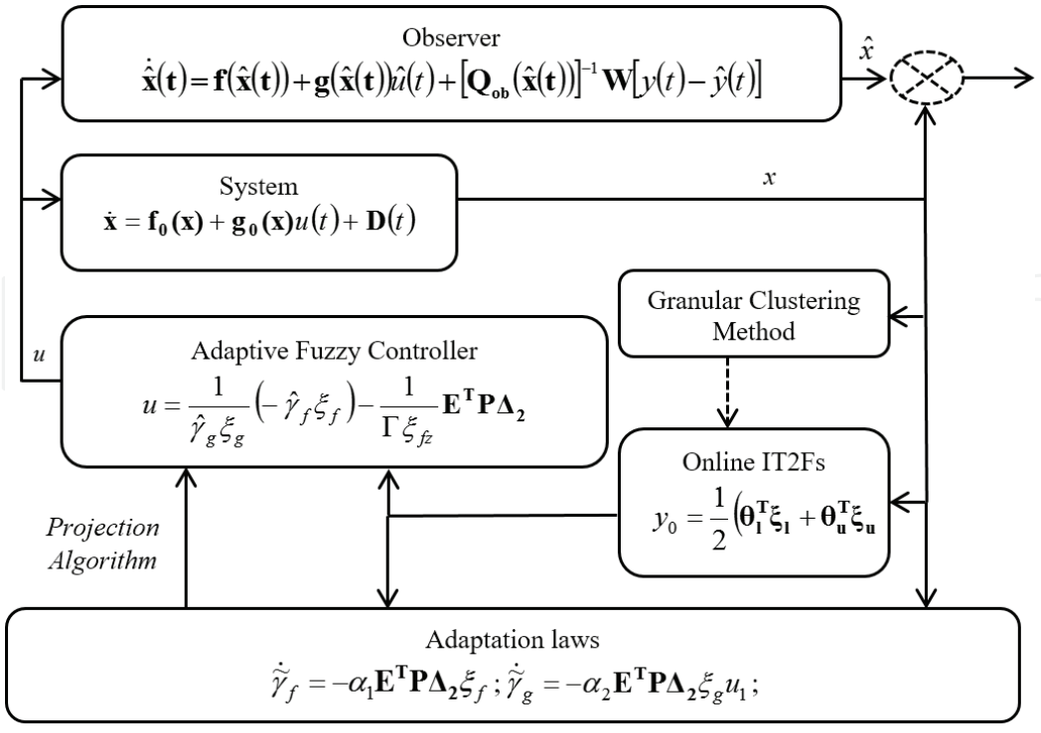

Figure 2. Control flow chart of the HAC-IFV.

4. Application to seat suspension system

4.1. Control results of the HAC-PP

In order to implement two adaptive controllers, principal parameters of the seat suspension and MR damper as shown in **Figure 3** are given in [25]. And two different road profiles of random step wave road and regular bump road are adopted to emulate severe external disturbances as shown in **Figure 4**. The first excitation is collected from the real road, and the second excitation is used same as in [25]. The process of simulation is expressed as follows: The proposed control will be simulated following an objective trajectory, which is control of [25]. Then, the outputs of the proposed control and the objective will be used for calculating error. This error will be checked by desired prescribed performance. It is remarked that the desired prescribed performance is different from the applied prescribed performance which is shown

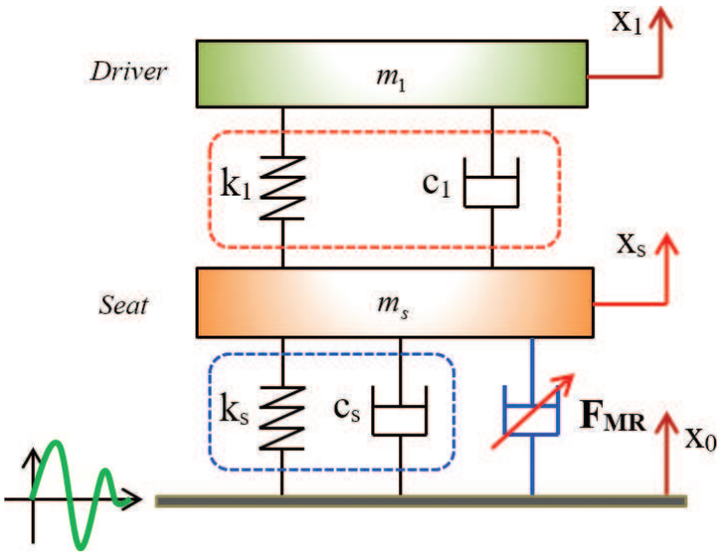

Figure 3. Mechanical model of a vehicle seat suspension system.

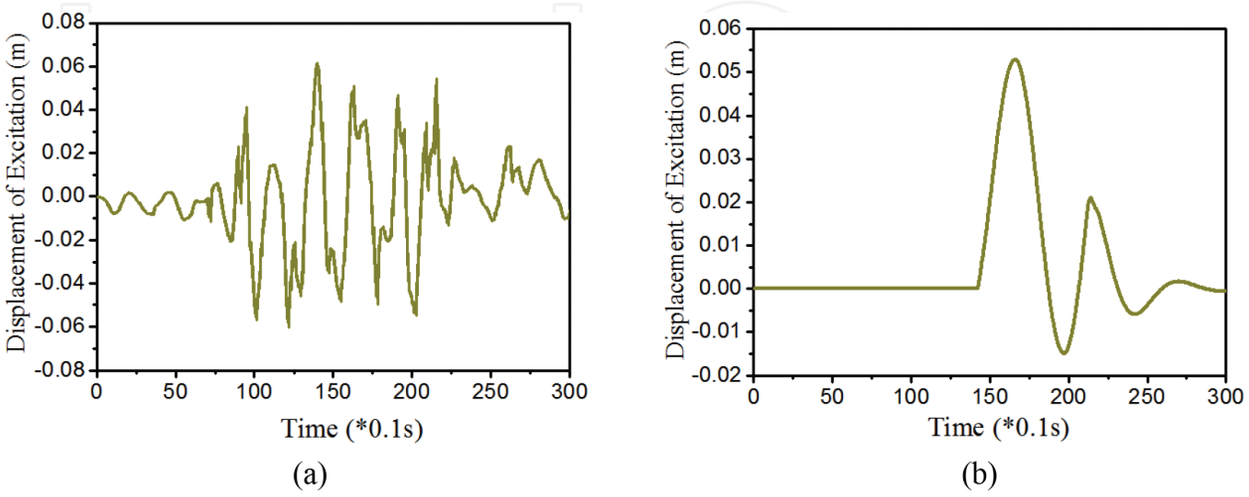

Figure 4. Road excitation signals: (a) random step wave road, (b) regular-bump road.

in Eqs. (7)–(13). The parameters of both the desired and the applied prescribed performance are listed in **Table 1**. The damping force of the MR damper is designed 1000 N (±5%) at 2 A. The fuzzy model is established based on the online model with the centroid vector as shown in [25]. It is noted that two main variables for the fuzzy models are displacement and acceleration. The fuzzy models include 6 clusters, and then the outputs of fuzzy rules become also 6. The sigma value for Gaussian function of the fuzzy model is chosen as 0.4 [22, 25], and this value is not changed through the simulation. The values of the sliding surface $[k_1, k_2]$ are chose by [1, 20] for both random step wave road and regular bump road. The constant value Γ of the

Parameter	Desired prescribed performance	Applied prescribed performance
Initial value $\lambda(0)$	0.5	0.5
Infinity value λ_∞	0.001	0.001
Exponential value l	1	0.00047

Table 1. Parameters of desired prescribed performance and applied prescribed performance.

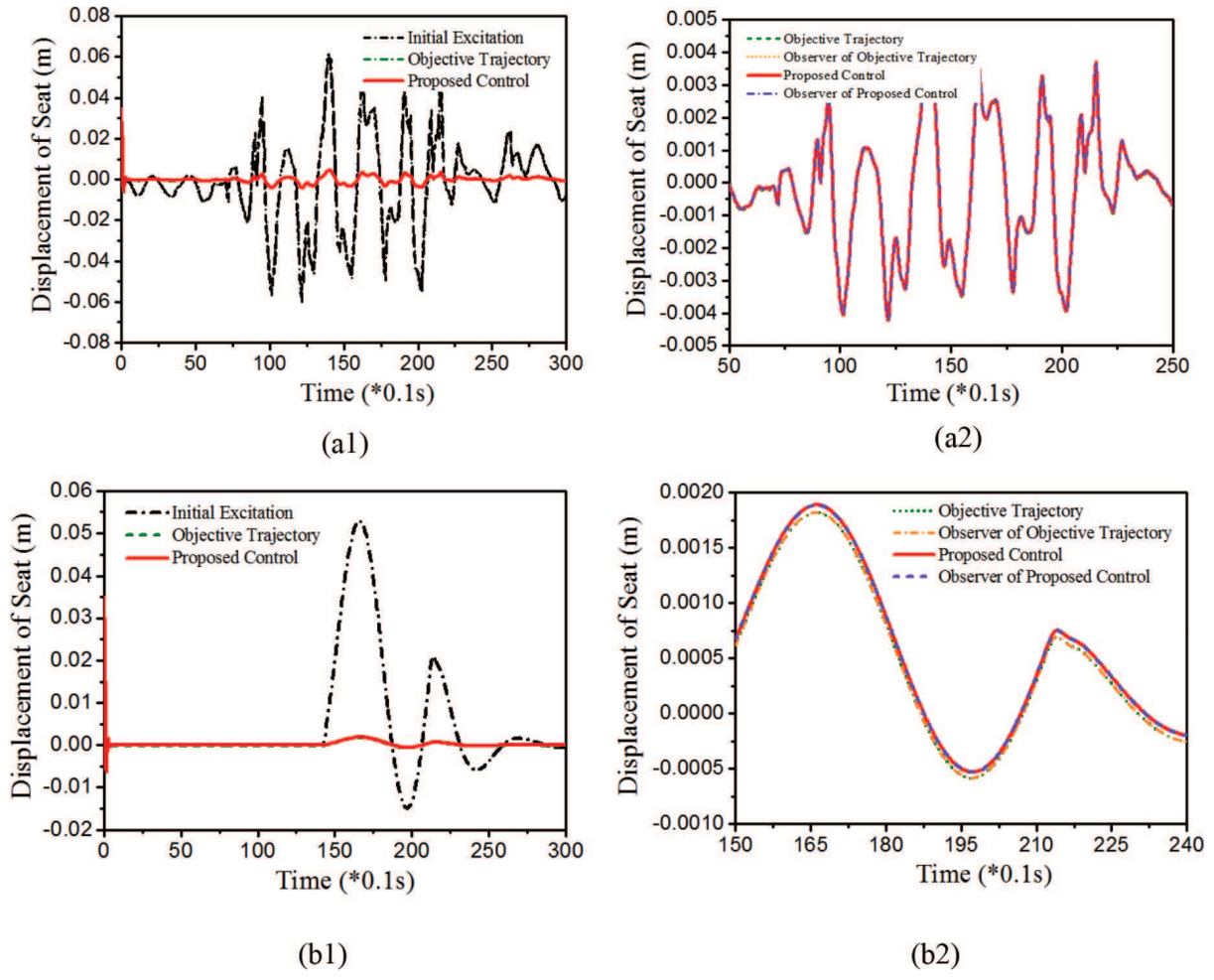

Figure 5. Control results with the HAC-PP at the seat (x_s): (a1, a2) random step wave road, (b1, b2) regular bump road.

Riccati-like equation is chosen by 10 for both roads. The constant c_s is 500 and 5000 for regular bump road and the random step wave road, respectively. In addition, the matrix $\mathbf{Q}$ of the Riccati-like equation is chosen as $\mathbf{Q}=[-2 \quad 0; 0 \quad -2]$. The constants μ_1, μ_2, μ_3 of adaptation laws are chosen as 10 for two road profiles. The values of $\aleph_f$, $\aleph_g$, $\Theta\Gamma$ of the expanded adaptation laws are chosen by 0.1 and the values of δ_1, δ_2, δ_3 are chosen by 0.1. In this simulation, the initial states for the dynamic states are used as $[0.035 \quad 2.5]$, $[0.035 \quad 2.5]$ for random regular bump, and random step wave bump, respectively. The initial states for the observer are $[0.035 \quad 0]$ for two excitations. It is noted that the observer is applied to evaluate the results of the proposed controller.

Figures 5–8 present control responses of the HAC-PP. It is clearly observed from **Figures 5** and **6** that the initial excitation has been significantly reduced by activation the proposed adaptive controller in terms of both displacement and acceleration. In addition, it is seen that the proposed control well tracks the objective trajectory which directly indicates high performance of the prescribed performance of the sliding surface. **Figure 7** presents the error of performance of the proposed adaptive controller which is always less than the boundary of the prescribed

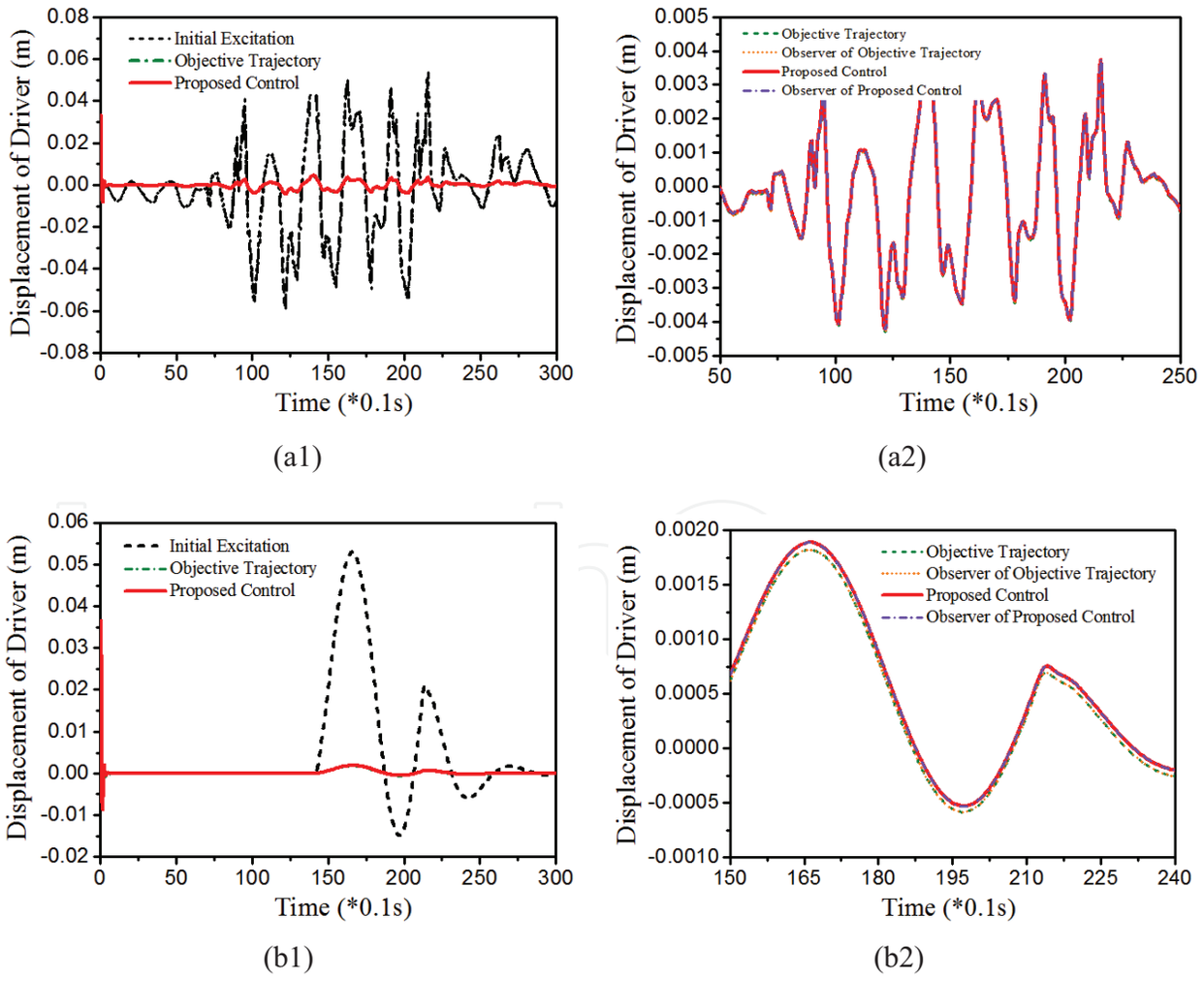

Figure 6. Control results with the HAC-PP at the driver (x_1): (a1, a2) random step wave road, (b1, b2) regular bump road.

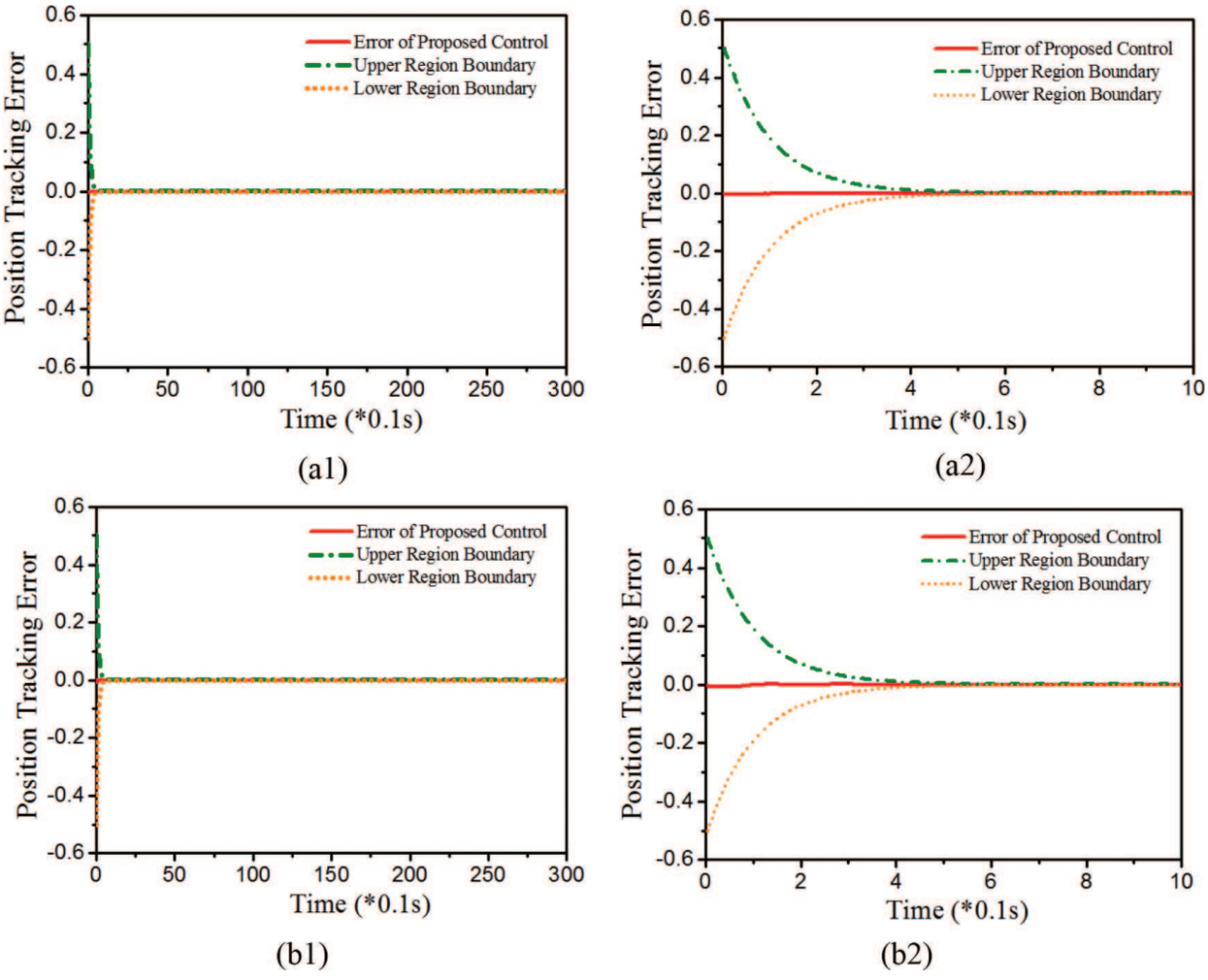

Figure 7. Tracking error with the HAC-PP: (a1, a2) random step wave road, (b1, b2) regular bump road.

performance. These results mean that the application of the prescribed performance in design of the hybrid adaptive controller can improve the quality of control with high robustness against severe excitations.

4.2. Control results of the HAC-IFV

In simulation of the HAC-IFV, the values of the sliding surface $[k_1, k_2]$ are chosen by $[1, 1.10^{-5}]$. The constant value Γ of the Riccati-like equation is chosen by 40, 10 for the regular bump road, the random step wave road, respectively. The constants α_1, α_2 of adaptation laws are chosen as 10 for all road profiles. The values of ε_f, ε_g of the expanded adaptation laws are chosen by 10 and the values of δ_1, δ_2 are chosen by 0.05. In this simulation, the initial states for the dynamic states are used as $[0.122 \quad 2.5]$, $[0.066 \quad 2.5]$, $[0.047 \quad 2.5]$ for random bump, random regular bump, and random step wave bump, respectively. The initial states for the observer are $[0.06 \quad 0]$ for two excitations. It is noted that the observer is applied to evaluate the results of the proposed controller. The parameters $[k_1, k_2]$ are chosen as [1, 1.5] for random regular bump and [1, 5] for random step wave bump.

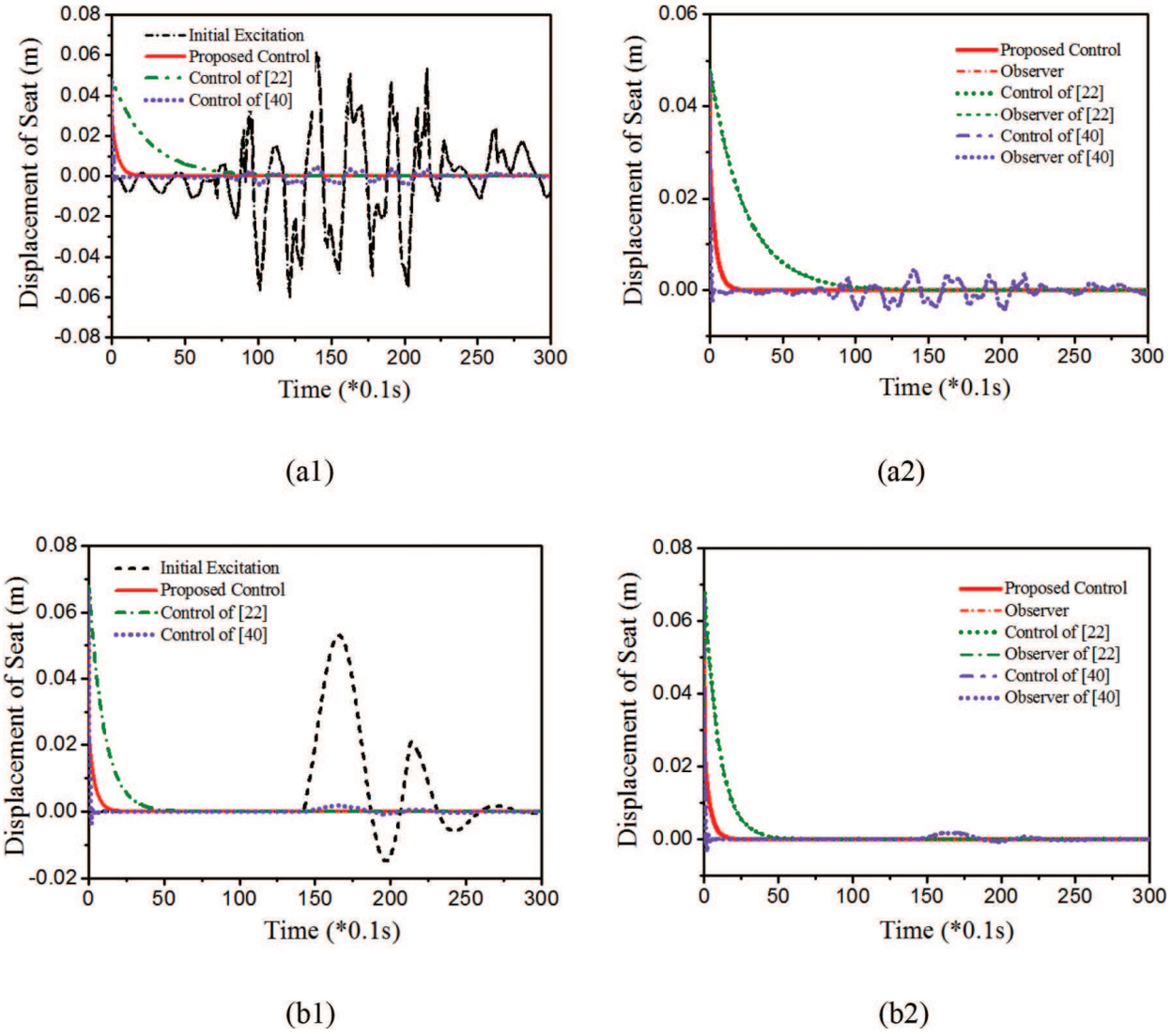

Figure 8. Control results with the HAC-IFV at the seat (x_s): (a1, a2) random step wave road, (b1, b2) regular bump road.

Figures 8–10 present control responses of the HAC-IFV. As similar to the HAC-PP, the initial excitations were remarkably reduced by applying the proposed controller. The displacements at the seat and driver positions are reduced resulting in the improvement of the ride comfort. In order to demonstrate a salient benefit of the proposed controller, its control response is compared obtained from the controller proposed in [17, 25]. It is clearly identified that the convergence time of the displacement of the proposed controller is 2 seconds for both excitations, while that is 15 seconds for the random step wave excitation, 6 seconds for regular bump excitation in [17, 25]. In **Figure 8**, the sliding surfaces of three controllers are shown. It is observed that the proposed control obtains stable motion much faster than the comparative controls at 0.1 second. It is noted here that the better control responses of the proposed controller comes from the inversely fuzzified values in given Eqs. (46)–(48). In Eq. (48), the independent of the inversely fuzzified value helps the controller to increase its robustness. This new exploration is the outstanding property of the proposed controller in the severe operation environment subjected to strong and random disturbances.

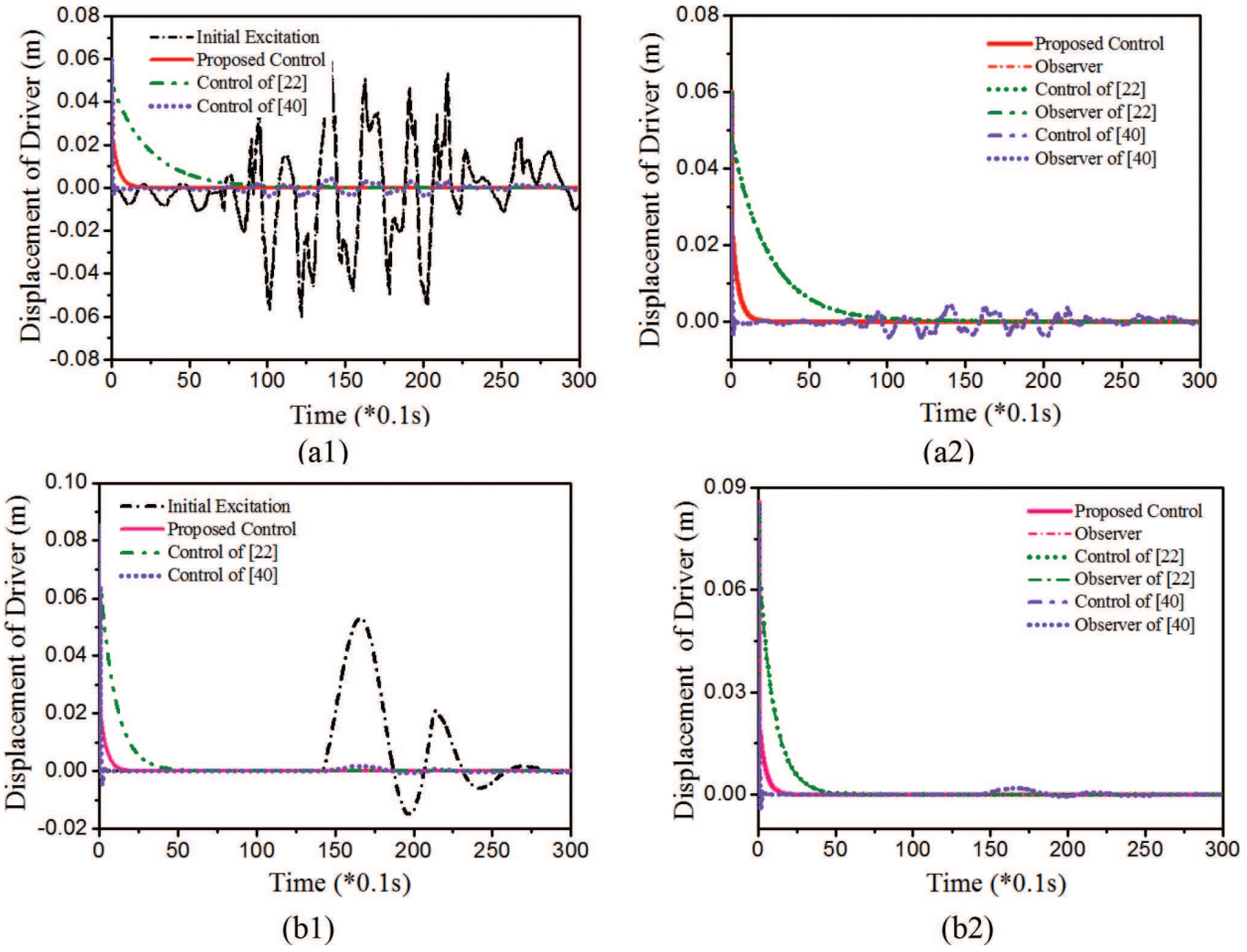

Figure 9. Control results with the HAC-IFV at the driver (x_1): (a1, a2) random step wave road, (b1, b2) regular bump road.

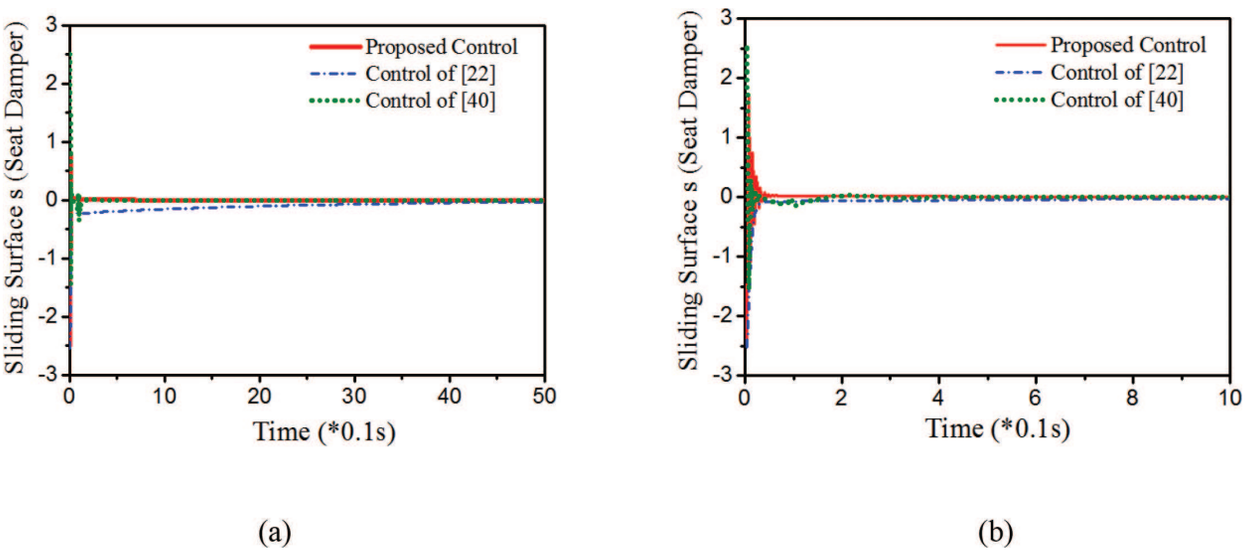

Figure 10. Sliding surface motion of the HAC-IFV (s): (a) random step wave road, (b) regular bump road.

5. Concluding remarks

In this study, two new adaptive controllers were formulated and their effectiveness was validated by applying them to vibration control of a semi-active vehicle seat suspension system featuring MR damper. The first adaptive controller includes two sliding mode controls: one for initial states of the system and the other for prescribed performance associated with the parameters of the modified Riccati-like equation. By doing this way, the tracking performance is enhanced resulting in the improved control responses. The second adaptive controller was formulated on the basis of the inversely fuzzified value with the H-infinity control to minimize computational cost algorithm. Hence, by doing this way, the convergence time can be reduced resulting in high stability of the system subjected to severe external disturbances. It has been sown that the proposed two adaptive controllers can significantly reduce the excitation from the road profiles at both the seat and driver positions. In reality, this can enhance the ride comfort of the driver. Especially, the HAC-PP provides good tracking performance with the error in range of the defined boundary and the HAC-IFV can reduce the convergence time compared with two comparative adaptive controllers. It is finally remarked that the development of a new hybrid adaptive controller needs to be connected with desired control performances to appropriately select each control scheme.

Acknowledgements

This research was funded by Vietnam National Foundation for Science and Technology Development (NAFOSTED) under grant number 107.01-2017.28. The financial support is gratefully acknowledged.

Declaration of conflicting interest

The authors declare that there is no conflict of interest.

Author details

Do Xuan Phu[1], Ta Duc Huy[1] and Seung Bok Choi[2]*

*Address all correspondence to: seungbok@inha.ac.kr

1 MediRobotics Laboratory, Department of Mechatronics and Sensor System Technology, Vietnamese-German University, Binh Duong, Vietnam

2 Smart Structures and Systems Laboratory, Department of Mechanical Engineering, Inha University, Incheon, Korea

References

[1] Shahriari Kahkeshi M, Sheikholeslam F, Zekri M. Design of adaptive fuzzy wavelet neural sliding mode controller for uncertain nonlinear systems. ISA Transactions. 2013;**52**:342-350

[2] Do XP, Shah K, Choi S-B. Damping force tracking control of MR damper system using a new direct adaptive fuzzy controller. Shock and Vibration. 2015;**2015**:947937

[3] Huang S-J, Chen H-Y. Adaptive sliding controller with self-tuning fuzzy compensation for vehicle suspension control. Mechatronics. 2006;**16**:607-622

[4] Shahnazi R. Output feedback adaptive fuzzy control of uncertain MIMO nonlinear systems with unknown input nonlinearities. ISA Transactions. 2015;**54**:39-51

[5] Cui Y, Zhang H, Wang Y, Zhang Z. Adaptive neural dynamic surface control for a class of uncertain nonlinear systems with disturbances. Neurocomputing. 2015;**165**:152-158

[6] Wu L-B, Yang G-H. Adaptive fuzzy tracking control for a class of uncertain non-affine nonlinear systems with dead-zone inputs. Fuzzy Sets and Systems. 2015;**290**:1-21

[7] Hsu C-F. Adaptive fuzzy wavelet neural controller design for chaos synchronization. Expert Systems with Applications. 2011;**38**:10475-10483

[8] Li Y, Tong S. Prescribed performance adaptive fuzzy output-feedback dynamic surface control for nonlinear large-scale systems with time delays. Information Sciences. 2015;**292**: 125-142

[9] Huang Y, Na J, Wu X, Liu X, Guo Y. Adaptive control of nonlinear uncertain active suspension systems with prescribed performance. ISA Transactions. 2015;**54**:145-155

[10] Yi-Min L, Yang Y, Li L. Adaptive backstepping fuzzy control based on type-2 fuzzy system. Journal of Applied Mathematics. 2012;**2012**:658424

[11] Gao Y, Er MJ. Online adaptive fuzzy neural identification and control of a class of MIMO nonlinear systems. IEEE Transactions on Fuzzy Systems. 2003;**11**(4):462-477

[12] Lin F-J, Chou P-H, Shieh P-H, Chen S-Y. Robust control of an LUSM-based X-Y-θ motion control stage using an adaptive interval type-2 fuzzy neural network. IEEE Transactions on Fuzzy Systems. 2009;**17**(1):24-38

[13] Wang F, Liu Z, Zhang Y, Chen CLP. Adaptive fuzzy control for a class of stochastic pure-feedback nonlinear systems with unknown hysteresis. IEEE Transactions on Fuzzy Systems. 2016;**24**(1):140-152

[14] Phu DX, Choi S-B. Vibration control of a ship engine system using high-load magnetorheological mounts associated with a new indirect fuzzy sliding mode controller. Smart Materials and Structures. 2015;**24**:025009

[15] Choi S-B, Li W, Yu M, Du H, Fu J, Do PX. State of the art of control schemes for smart systems featuring magneto-rheological materials. Smart Materials and Structures. 2016;**25**: 043001

[16] Phu DX, Shin DK, Choi S-B. Design of a new adaptive fuzzy controller and its application to vibration control of a vehicle seat installed with an MR damper. Smart Materials and Structures. 2015;**24**:085012

[17] Phu DX, Shah K, Choi S-B. Design of a new adaptive fuzzy controller and its implementation for the damping force control of a magneto-rheological damper. Smart Materials and Structures. 2014;**23**:065012

[18] Phu DX, Choi S-B, Lee Y-S, Han M-S. Vibration control of a vehicle's seat suspension featuring a magneto-rheological damper based on a new adaptive fuzzy sliding-mode controller. Proceedings of the Institution of Mechanical Engineers, Part D: Journal of Automobile Engineering. 2015;**230**(4):437-458. DOI: 10.1177/0954407015586678

[19] Fayek HM, Elamvazuthi I, Perumal N, Venkatesh B. A controller based on optimal type-2 fuzzy logic: Systematic design, optimization and real-time implementation. ISA Transactions. 2014;**53**:1583-1591

[20] Wang X, Liu X, Zhang L. A rapid fuzzy rule clustering method based on granular computing. Applied Soft Computing. 2014;**24**:534-542

[21] Mendel JM, Liu X. Simplified interval type-2 fuzzy logic systems. IEEE Transactions on Fuzzy Systems. 2013;**21**(6):1056-1069

[22] Juang C-F, Tsao Y-W. A self-evolving interval type-2 fuzzy neural network with online structure and parameter learning. IEEE Transactions on Fuzzy Systems. 2008;**16**(6):1411-1424

[23] Liu J. Sliding Mode Control Using MATLAB. Academic Press: Tsinghua University Press; 2017

[24] Ciccarella G, Dalla Mora M, Germani A. A Luenberger-like observer for nonlinear systems. International Journal of Control. 1993;**57**(3):537-556

[25] Phu DX, Choi S-M, Choi S-B. A new adaptive hybrid controller for vibration control of a vehicle seat suspension featuring MR damper. Journal of Vibration and Control. 2016: 1-22. DOI: 10.1177/1077546316629597

IntechOpen